

Enhanced Magnetization in Proton Irradiated $\text{Mn}_3\text{Si}_2\text{Te}_6$ van der Waals Crystals

L. M. Martinez¹, H. Iturriaga¹, R. Olmos¹, L. Shao², Y. Liu³, Thuc T. Mai⁴, C. Petrovic³, Angela R. Hight Walker⁴, and S. R. Singamaneni^{1*}

¹Department of Physics, The University of Texas at El Paso, El Paso, Texas 79968, USA

²Department of Nuclear Engineering, Texas A&M University, College Station, TX 77845, USA

³Condensed Matter Physics and Materials Science Department, Brookhaven National Laboratory, Upton, New York 11973, USA

⁴Nanoscale Device Characterization Division, Physical Measurement Laboratory, National Institute of Standards and Technology, Gaithersburg, Maryland 20899, USA

Abstract

van der Waals (vdW) engineering of magnetism is a topic of increasing research interest in the community at present. We study the magnetic properties of quasi-two-dimensional layered vdW $\text{Mn}_3\text{Si}_2\text{Te}_6$ (MST) crystals upon proton irradiation as a function of fluence 1×10^{15} , 5×10^{15} , 1×10^{16} , and 1×10^{18} H^+/cm^2 . We find that the magnetization is significantly enhanced by 53% and 37% in the ferrimagnetic phase (at 50 K) when the MST was irradiated with the proton fluence of 5×10^{15} , both in *ab* and *c* plane, respectively. The ferrimagnetic ordering temperature and magnetic anisotropy are retained even after proton irradiation. From the fluence dependence of magnetization, electron paramagnetic resonance spectral parameters (*g*-value and signal width), and Raman data, we show that the magnetic exchange interactions (Mn-Te-Mn) are significantly modified at this fluence. This work shows that it is possible to employ proton irradiation in tuning the magnetic properties of vdW crystals, and provide many opportunities to design desired magnetic phases.

*srao@utep.edu

The manipulation of the physical properties of materials through irradiation or photo-excitation has been of particular interest for electronic device functionality in space¹⁻³, and the fundamental understanding of the interaction between light and matter⁴⁻⁷, respectively. In particular, proton irradiation is known as one of the main sources that hinders the electrical properties of electronics in space-crafts undergoing tasks near earth's orbit^{8,9}. However, proton irradiation has the potential to positively impact the magnetic characteristics of materials¹⁰. Studies have shown that irradiation with protons induces ferromagnetic ordering in some materials such as MoS₂ and graphite, materials that are normally non-magnetic¹¹⁻¹⁹. For example, MoS₂ has been a popular van der Waals (vdW) material to study due to its similarities to graphene, while maintaining the benefits of a large direct band gap (1.8 eV), good electrical properties and catalytic activity²⁰⁻²⁴. Using proton irradiation, Mathew *et al.*¹⁶ introduced magnetic ordering in MoS₂, which resulted in a change from diamagnetic to ferrimagnetic behavior above room temperature, attributed to vacancies and edge states produced by proton irradiation. Another study by Wang *et al.* shows a change in the bandgap of MoS₂ due to defects that trap excitons after irradiation¹. In the case of graphite, exposure to irradiation¹¹ yielded ferromagnetic ordering.

vdW materials have recently risen in interest due to the ability of exfoliating the bulk crystals down to a few- or mono-layers and still retain and/or improve their pristine magnetic properties²⁵⁻²⁸. Even though many studies have emerged on these vdW materials, there are various materials, in that family, that have remained less explored in bulk or few-layer form. Mn₃Si₂Te₆ (MST), similar to Cr₂Si₂Te₆ (CST), which is another vdW magnet, is a part of the vdW family of layered materials that has only recently received some renewed interest^{29,30}. May and co-authors³⁰ determined the trigonal crystal structure, containing MnTe₆ octahedra that share edges within the *ab*-plane (Mn1 site). In MST, one third of the Mn atoms link the layers together by filling the

octahedral holes (Mn2 site) within the vdW gap, and these two sites are antiferromagnetically aligned. Later on, Liu and Petrovic performed a study²⁹ on the critical behavior of MST and confirmed a ferrimagnetic temperature (T_c) of ~ 74 K.

To date, various strategies such as electrostatic gating, pressure and iso-valent alloying have been employed to control magnetism in 2D layered magnets. Using proton irradiation, we hope to modify the magnetic properties of MST as a function of proton fluence, which was unreported earlier. However, proton irradiation is uncommon on Earth, but represents the majority of cosmic radiation incident to the Earth's atmosphere. Studying the effects of proton irradiation on vdWs materials can give clues as to their general behavior when irradiated in space environments as exemplified in recent reviews^{31,32} and report.³³

In this study, we irradiated MST with protons at an energy of 2 MeV at the different proton fluence of 1×10^{15} , 5×10^{15} , 1×10^{16} and 1×10^{18} H^+/cm^2 . A non-linear change in the magnetization (measured from hysteresis loops) was observed as a function of proton fluence. We noticed no dramatic change in T_c upon proton fluence. Electron paramagnetic resonance (EPR) measurements show two signals corresponding to Mn^{2+} paramagnetic centers, assigned to Mn1 and Mn2 sites. No additional signals were observed indicating the absence of magnetic defects that may have been formed after irradiation. EPR data coupled with the Raman data suggests that the proton irradiation modify the exchange interactions in MST and may have played a key role in the modification of the magnetization.

MST single crystals (mm in lateral dimensions, < 0.5 mm in thickness) were prepared as reported previously by some of us (Y.L and C.P)²⁹. A Quantum Design Versalab System with a temperature range of 50 – 400 K and magnetic field range of ± 3 T was used for this study. The magnetic field was applied in the ab plane, as well as in the c plane. The EPR spectra were recorded

on a Bruker EMX Plus X-band (~9.43 GHz) spectrometer, equipped with a high sensitivity probe head. A Cold-Edge™ ER 4112HV In-Cavity Cryo-Free VT system connected with an Oxford temperature measurement was used in combination with the EPR spectrometer. All the samples were carefully handled with nonmagnetic capsules and Teflon tapes to avoid contamination. The 2 MeV proton irradiation was performed by using a 1.7 MV Tandatron accelerator. This energy was chosen to avoid producing unwanted damage in the crystal. The projected range was 30 microns, and the damage profile has a relative flat distribution from the surface up to 30 microns (supplementary materials [SM], Figure S1). The beam current was 100 nA. The beam spot size was 6mm × 6mm and the beam was rastered over an area of 1.2 cm x 1.2 cm to guarantee lateral beam uniformity. The weak beam current and the beam rastering reduce the beam heating (< 50°C) during the irradiation. The beam was filtered with multiple magnet bending devices to remove carbon contamination^{34,35}. The vacuum during the irradiation was 6E⁻⁸ Torr or better. The application of liquid nitrogen trapping during irradiation was performed to improve vacuum. The proton irradiation was carried out on separate crystals for each fluence. Raman spectra were collected in parallel geometry using a Renishaw Raman spectrometer using 532 nm laser wavelength excitation with 15s count and 50x optical microscope objective.

To study the variation of magnetization as a function of proton fluence, the isothermal (50 K) magnetization measurements were performed as a function of proton fluence, both in the *ab* and *c* plane in the ferrimagnetic phase, and the data are plotted in Fig. 1 (a,b). To compare, isothermal magnetization variation for the pristine crystal (shown with the curve in black) in both the directions is also included. As shown in Fig. 1(a) for *ab* plane, square-shaped M-H loops are observed at all the fluences, associated with negligible coercive field, consistent with the previous reports^{29,30}. Most interestingly, the *ab* plane magnetization observed at 50 K is enhanced by about

53% when the MST crystal was irradiated with the proton fluence of $5 \times 10^{15} \text{ H}^+/\text{cm}^2$, in comparison with that of pristine crystal. A similar trend is observed even when the magnetization was measured in the c plane as depicted in Fig. 1 (b) as the magnetization in the c plane is known^{29,30} to have small ferromagnetic contribution. Figure 1 (a,b) shows that the strong magnetic anisotropy is retained even after the proton irradiation. The magnetization in ab plane is higher than the c plane as ordered moments lie primarily within the ab plane in agreement with the previous reports on MST^{29,30}. No remanent moment for either orientation confirms the crystal retains its high quality even after the proton irradiation.

The trends in the magnetization as a function of proton fluence are captured in Fig. 1 (c), both for ab and c plane magnetization. As it can be immediately evidenced, the highest magnetization value was observed for the isothermal magnetization measurement irradiated with a proton fluence of $5 \times 10^{15} \text{ H}^+/\text{cm}^2$, with an increase of 53% with respect to its pristine value. The magnetization decreased when MST was irradiated with a fluence of 1×10^{16} and $1 \times 10^{18} \text{ H}^+/\text{cm}^2$. Here, the magnetization value is taken for all the samples measured at 50 K and 3 T from Fig. 1(a,b).

To study T_c as a function of proton fluence, the temperature dependent magnetization measurements were performed, both in the ab and c plane, plotted in the SM, Figure S2 (a, b). The dM/dT (Fig. 2) curves show no significant change in T_c upon proton irradiation. In the pristine MST, the T_c was found at ~ 74 K, in good agreement with previous reports^{29,30}. The most noticeable change in the T_c was observed after a proton fluence of $1 \times 10^{18} \text{ H}^+/\text{cm}^2$ with a small decrease of 1.4 K (SM, Table S1). The $1/\chi$ vs. T plots (SM, Fig. S3) were fitted using the Curie-Weiss law, $\chi = C/(T-\theta_w)$, in order to extract the Weiss temperature (θ_w). The fits were done with the temperature range of 200-400 K, and the resulting θ_w values are displayed in SM, Table S1.

The extracted T_c was found to be negative indicating antiferromagnetic correlations³⁰ and almost three times greater than the T_c estimated from dM/dT curves. The effective moment is consistent with the presence of Mn^{2+} ions, also supported by EPR measurements (see below). The deviation from the T_c points toward short-range spin correlations that exist in MST³⁰. Consistent with the MH data, the magnetization in ab plane is higher than in the c plane as expected^{29,30}. For comparison, the temperature dependent magnetization data collected on the pristine crystal is also included as shown in black curve.

To gain insights into the origin of enhancement in the magnetization at the fluence of 5×10^{15} , the temperature dependent EPR measurements were performed across T_c . EPR is an ideal tool to identify paramagnetic centers that contain unpaired electron spins, local environments, and possible magnetic secondary phases by studying the temperature dependent EPR spectral parameters such as g -value and signal width³⁶⁻⁴². The EPR spectra collected on all the compounds in the ferrimagnetic phase at 50 K are plotted in Fig. 3, which includes both the experimental (dotted curve) as well as the computer-generated fits (continuous curve) using the Lorentzian and Dysonian line shapes (SM, Fig. S4). From the fits, we identified two overlapped signals. The EPR spectral parameters such as the signal width and g -value (including those of pristine MST) were extracted from the fits and are plotted as a function of fluence (SM, Fig. S5). Upon closer inspection, a clear variation in the EPR spectral parameters is noticed at around the fluence of $5 \times 10^{15} \text{ H}^+/\text{cm}^2$. At that fluence, the linewidth for both the signals shows a minimum due to strong exchange narrowing effect⁴³; and the g -value is maximum due to the local enhanced magnetic corrections⁴⁴.

Now, we will assign the two EPR signals. Previous reports^{29,30} show that this compound has two Mn sites, namely, Mn1 (in ab plane) and Mn2 (in c plane). It is also known that the

multiplicity of Mn1 is twice that of Mn2 and are significantly separated through distance. That means the magnetic moment of Mn1 is expected to be two times higher than Mn2. The first Mn site (Mn1 site) is composed of MnTe₆ octahedra that are edge-sharing within the *ab*-plane. The Mn2 site links the layers together by filling one-third of the octahedral holes within the vdW gap³⁰. Due to strong exchange interaction (Mn1-Mn1 ~ 4.06 A⁰) among the spins on Mn1 site, the EPR signal width is expected to be smaller. Hence, it is reasonable to assign the sharper signal ($\Delta H_{PP} \sim 180\text{-}200$ G) to Mn1. On the other hand, the broader signal ($\Delta H_{PP} \sim 1200\text{-}1800$ G) can be assigned to Mn2 site. The different surroundings of these two Mn sites produce EPR signals associated with distinct spectral properties. The main signal is sharper, intense, and associated with the g-value of 1.998. The broader signal is less intense, associated with $g \sim 1.85$. Two EPR signals were also observed in the paramagnetic phase (80 K) (SM, Fig. S6). Besides the Mn²⁺ signals ($S = 5/2$; $L = 0$), no additional signals related to (magnetic) defects were observed after proton irradiation. This indicates that the observed changes in magnetization is not due to magnetic defects produced after irradiation. Additionally, hydrogen ion implantation can be ruled out as a likely cause to the change in magnetization because of a lack of hyperfine structures¹² in our EPR spectra of the proton irradiated MST crystals. Fluence dependent magnetic properties were also reflected from the magneto caloric effect measurements (SM, Fig. S7).

To study the effect of proton irradiation on the lattice vibrations, we performed Raman spectroscopic measurements before and after the irradiation as shown in Fig. 4 (a). The peak position as a function of proton fluence, extracted from the fits, is plotted in Fig. 4 (b). The Raman spectra for MST has not been previously reported in the literature. However, the Raman spectra for its analogues compound CST is reported^{45,46} with peaks arising from the in-plane and out-of-plane Te vibrational modes, which are sensitive to magnetic interactions. The modes seen in the

MST Raman spectra located at 118.4 cm^{-1} with a shoulder at 136.9 cm^{-1} are close to the peaks found for CST for the E_g^3 and A_g^3 modes^{45,46}, respectively. The main difference in the spectra of MST and CST arises from the change in mass and lattice parameter effects that cause the phonon positions to be slightly different. From Fig. 4 (b), the change in the E_g peak as a function of fluence mimics the observed trend in the M_s shown in Fig. 1 (c). Thus, it is very likely the E_g^3 and A_g^3 modes involve atomic motions of the Te atoms whose bond strength can be very susceptible to the spin interactions, since the Te atoms mediate the super-exchange between the two Cr atoms. *While our initial temperature dependent Raman data (SM, Fig. S8) show changes in spectral parameters, indicative of the modification in spin-lattice coupling upon proton irradiation, other factors such as changes at local band structure and surface crystal structure could also be at play.*

It is more likely that the proton irradiation produced changes in the magnetic interactions within MST. As mentioned before, MST has been shown to contain competing antiferromagnetic interactions that create frustration within the system³⁰. In particular, the Mn1-Mn1 interactions were reported to have a rivalry between direct interaction (AFM) and Mn1-Te-Mn1 interactions that can lead to FM or AFM which is determined by whether or not the p or d orbitals are participating³⁰. A recent archived report by Ron *et al.*, studied the ligand-to-metal charge transfer (CT) in CrSiTe_3 ⁴⁷. This was achieved by targeting specific CT transitions in CST using ultrafast laser pulses. They find that by targeting these CT transitions, an enhancement in the nearest-neighbor super-exchange interactions occurs, weakening the AFM direct exchange, and thus resulting in an increase in FM exchange. Upon proton irradiation, it is most likely that competing magnetic interactions could be affected by varying the fluence of protons and caused the change in magnetization.

To conclude, we report that the magnetization is significantly enhanced by 53% and 37% in ferrimagnetic phase when the MST was irradiated with the proton fluence of 5×10^{15} , in the *ab* and *c* plane respectively. From the results obtained from fluence dependent magnetic, EPR and Raman spectroscopic measurements, we show that the magnetic exchange interactions (Mn-Te-Mn) are modified at this fluence. This work signifies that proton irradiation is very effective in tuning the magnetism of vdW crystals.

Supplementary Material

See supplementary material for the proton irradiation depth profile and temperature dependent magnetization measurements performed in both crystallographic directions (*H//ab* and *H//c*). The χ^{-1} vs. Temperature curves are presented with their respective CW fits. EPR analysis of the individual signal spectra, at 50 K, for each irradiated crystal along with the pristine crystal is presented. Additionally, the EPR spectra measured at 80 K is also shown with the change in *g*-value and linewidth, of both signals, as a function of proton fluence. The change in the magnetic entropy is also presented as a function of proton fluence. Lastly, low temperature Raman measurements of the pristine and an irradiated crystal (1×10^{18} H⁺/cm²) is presented along with an analysis of the Raman spectra.

L.M.M acknowledges the useful discussions with H. S. Nair. L.M.M and S.R.S acknowledge support from a UTEP start-up grant. L.M.M acknowledges the Wiemer Family for awarding Student Endowment for Excellence, and NSF-LSAMP Ph.D. Fellowship. This publication was prepared by S. R. Singamaneni and co-authors under the award number 31310018M0019 from The University of Texas at El Paso (UTEP), Nuclear Regulatory Commission. The Statements, findings, conclusions, and recommendations are those of the author(s) and do not necessarily reflect the view of the (UTEP) or The US Nuclear Regulatory Commission. Work at Brookhaven National Laboratory is supported by the Office of Basic Energy Sciences, Materials Sciences and Engineering Division, U.S. Department of Energy (DOE) under Contract No. DE-SC0012704. Authors thank S. R. J. Hennadige for his help in EPR measurements. T.T.M. and A.R.H.W.

acknowledge the National Institute of Standards and Technology (NIST)/National Research Council Postdoctoral Research Associateship Program and NIST-STRS (Scientific and Technical Research and Services) for funding. Certain commercial equipment, instruments, or materials are identified in this paper in order to specify the experimental procedure adequately. Such identification is not intended to imply recommendation or endorsement by the National Institute of Standards and Technology, nor is it intended to imply that the materials or equipment identified are necessarily the best available for the purpose.

- ¹ B. Wang, S. Yang, J. Chen, C. Mann, A. Bushmaker, and S.B. Cronin, *Appl. Phys. Lett.* **111**, 131101 (2017).
- ² A. Geremew, F. Kargar, E.X. Zhang, S.E. Zhao, E. Aytan, M.A. Bloodgood, T.T. Salguero, S. Romyantsev, A. Fedoseyev, D.M. Fleetwood, and A.A. Balandin, *ArXiv:1901.00551 [Cond-Mat, Physics:Physics]* (2019).
- ³ R.C. Walker, T. Shi, B. Jariwala, I. Jovanovic, and J.A. Robinson, *Appl. Phys. Lett.* **111**, 143104 (2017).
- ⁴ H. Daubric, R. Berger, J. Kliava, G. Chastanet, O. Nguyen, and J.-F. Létard, *Phys. Rev. B* **66**, 054423 (2002).
- ⁵ M. Shirai, N. Yonemura, T. Tayagaki, K. Kan'no, and K. Tanaka, *Journal of Luminescence* **94–95**, 529 (2001).
- ⁶ T. Nakayama, O. Yanagisawa, M. Arai, and M. Izumi, *Physica B: Condensed Matter* **329–333**, 747 (2003).
- ⁷ S. Sasaki, Y.F. Zhang, O. Yanagisawa, and M. Izumi, *Journal of Magnetism and Magnetic Materials* **310**, 1008 (2007).
- ⁸ G. Yang, S. Jang, F. Ren, S.J. Pearton, and J. Kim, *ACS Appl. Mater. Interfaces* **9**, 40471 (2017).
- ⁹ C. Claeys and E. Simoen, *Radiation Effects in Advanced Semiconductor Materials and Devices* (Springer-Verlag, Berlin Heidelberg, 2002).
- ¹⁰ A.V. Krasheninnikov and K. Nordlund, *Journal of Applied Physics* **107**, 071301 (2010).
- ¹¹ P. Esquinazi, D. Spemann, R. Höhne, A. Setzer, K.-H. Han, and T. Butz, *Phys. Rev. Lett.* **91**, 227201 (2003).
- ¹² K.W. Lee and C.E. Lee, *Phys. Rev. Lett.* **97**, 137206 (2006).
- ¹³ S.W. Han, Y.H. Hwang, S.-H. Kim, W.S. Yun, J.D. Lee, M.G. Park, S. Ryu, J.S. Park, D.-H. Yoo, S.-P. Yoon, S.C. Hong, K.S. Kim, and Y.S. Park, *Phys. Rev. Lett.* **110**, 247201 (2013).
- ¹⁴ T.L. Makarova, A.L. Shelankov, I.T. Serenkov, V.I. Sakharov, and D.W. Boukhvalov, *Phys. Rev. B* **83**, 085417 (2011).
- ¹⁵ M.A. Ramos, J. Barzola-Quiquia, P. Esquinazi, A. Muñoz-Martin, A. Climent-Font, and M. García-Hernández, *Phys. Rev. B* **81**, 214404 (2010).
- ¹⁶ S. Mathew, K. Gopinadhan, T.K. Chan, X.J. Yu, D. Zhan, L. Cao, A. Rusydi, M.B.H. Breese, S. Dhar, Z.X. Shen, T. Venkatesan, and J.T.L. Thong, *Appl. Phys. Lett.* **101**, 102103 (2012).
- ¹⁷ H. Ohldag, P. Esquinazi, E. Arenholz, D. Spemann, M. Rothermel, A. Setzer, and T. Butz, *New J. Phys.* **12**, 123012 (2010).
- ¹⁸ R.-W. Zhou, X.-C. Liu, H.-J. Wang, W.-B. Chen, F. Li, S.-Y. Zhuo, and E.-W. Shi, *AIP Advances* **5**, 047146 (2015).
- ¹⁹ P. Esquinazi, R. Höhne, K.-H. Han, A. Setzer, D. Spemann, and T. Butz, *Carbon* **42**, 1213 (2004).

This is the author's peer reviewed, accepted manuscript. However, the online version of record will be different from this version once it has been copyedited and typeset.

PLEASE CITE THIS ARTICLE AS DOI: 10.1063/1.50002168

11

- ²⁰ T.-Y. Kim, K. Cho, W. Park, J. Park, Y. Song, S. Hong, W.-K. Hong, and T. Lee, *ACS Nano* **8**, 2774 (2014).
- ²¹ Y. Yu, S.-Y. Huang, Y. Li, S.N. Steinmann, W. Yang, and L. Cao, *Nano Lett.* **14**, 553 (2014).
- ²² S. Yan, W. Qiao, X. He, X. Guo, L. Xi, W. Zhong, and Y. Du, *Appl. Phys. Lett.* **106**, 012408 (2015).
- ²³ X. Ren, L. Pang, Y. Zhang, X. Ren, H. Fan, and S. (Frank) Liu, *J. Mater. Chem. A* **3**, 10693 (2015).
- ²⁴ L.M. Martinez, J.A. Delgado, C.L. Saiz, A. Cosio, Y. Wu, D. Villagrán, K. Gandha, C. Karthik, I.C. Nlebedim, and S.R. Singamaneni, *Journal of Applied Physics* **124**, 153903 (2018).
- ²⁵ P. Ajayan, P. Kim, and K. Banerjee, *Physics Today* **69**, 38 (2016).
- ²⁶ K.S. Burch, D. Mandrus, and J.-G. Park, *Nature* **563**, 47 (2018).
- ²⁷ D.L. Duong, S.J. Yun, and Y.H. Lee, *ACS Nano* **11**, 11803 (2017).
- ²⁸ A.F. May, D. Ovchinnikov, Q. Zheng, R. Hermann, S. Calder, B. Huang, Z. Fei, Y. Liu, X. Xu, and M.A. McGuire, *ACS Nano* (2019).
- ²⁹ Y. Liu and C. Petrovic, *Phys. Rev. B* **98**, 064423 (2018).
- ³⁰ A.F. May, Y. Liu, S. Calder, D.S. Parker, T. Pandey, E. Cakmak, H. Cao, J. Yan, and M.A. McGuire, *Phys. Rev. B* **95**, 174440 (2017).
- ³¹ R.C. Walker, T. Shi, E.C. Silva, I. Jovanovic, and J.A. Robinson, *Physica Status Solidi (a)* **213**, 3065 (2016).
- ³² A.V. Krasheninnikov and K. Nordlund, *Journal of Applied Physics* **107**, 071301 (2010).
- ³³ A. Geremew, F. Kargar, E.X. Zhang, S.E. Zhao, E. Aytan, M.A. Bloodgood, T.T. Salguero, S. Rummyantsev, A. Fedoseyev, D.M. Fleetwood, and A.A. Balandin, *ArXiv:1901.00551 [Cond-Mat, Physics:Physics]* (2019).
- ³⁴ L. Shao, J. Gigax, D. Chen, H. Kim, F.A. Garner, J. Wang, and M.B. Toloczko, *Nuclear Instruments and Methods in Physics Research Section B: Beam Interactions with Materials and Atoms* **409**, 251 (2017).
- ³⁵ J.G. Gigax, H. Kim, E. Aydogan, F.A. Garner, S. Maloy, and L. Shao, *Materials Research Letters* **5**, 478 (2017).
- ³⁶ C.L. Saiz, M.A. McGuire, S.R.J. Hennadige, J. van Tol, and S.R. Singamaneni, *MRS Advances* **4**, 2169 (2019).
- ³⁷ G.R. Haripriya, C.M.N. Kumar, R. Pradheesh, L.M. Martinez, C.L. Saiz, S.R. Singamaneni, T. Chatterji, V. Sankaranarayanan, K. Sethupathi, B. Kiefer, and H.S. Nair, *Phys. Rev. B* **99**, 184411 (2019).
- ³⁸ L.M. Martinez, C. Karthik, M. Kongara, and S.R. Singamaneni, *Journal of Materials Research* **33**, 1565 (2018).
- ³⁹ S.R. Singamaneni, J. van Tol, R. Ye, and J.M. Tour, *Appl. Phys. Lett.* **107**, 212402 (2015).
- ⁴⁰ H.S. Nair, R. Yadav, S. Adiga, S.S. Rao, J. van Tol, and S. Elizabeth, *Physica B: Condensed Matter* **456**, 108 (2015).
- ⁴¹ S.S. Rao, A. Stesmans, J. van Tol, D.V. Kosynkin, A. Higginbotham-Duque, W. Lu, A. Sinitiskii, and James.M. Tour, *ACS Nano* **6**, 7615 (2012).
- ⁴² S.S. Rao, A. Stesmans, D.V. Kosynkin, A. Higginbotham, and J.M. Tour, *New J. Phys.* **13**, 113004 (2011).
- ⁴³ P.M. Richards and M.B. Salamon, *Phys. Rev. B* **9**, 32 (1974).
- ⁴⁴ N.S. Sangeetha, S.D. Cady, and D.C. Johnston, *ArXiv:1809.02653 [Cond-Mat]* (2018).
- ⁴⁵ A. Milosavljević, A. Šolajić, J. Pešić, Y. Liu, C. Petrovic, N. Lazarević, and Z.V. Popović, *Phys. Rev. B* **98**, 104306 (2018).

This is the author's peer reviewed, accepted manuscript. However, the online version of record will be different from this version once it has been copyedited and typeset.

PLEASE CITE THIS ARTICLE AS DOI: 10.1063/1.50002168

⁴⁶ M.-W. Lin, H.L. Zhuang, J. Yan, T.Z. Ward, A.A. Puzos, C.M. Rouleau, Z. Gai, L. Liang, V. Meunier, B.G. Sumpter, P. Ganesh, P.R.C. Kent, D.B. Geohegan, D.G. Mandrus, and K. Xiao, *J. Mater. Chem. C* **4**, 315 (2015).

⁴⁷ A. Ron, S. Chaudhary, G. Zhang, H. Ning, E. Zoghlin, S.D. Wilson, R.D. Averitt, G. Refael, and D. Hsieh, ArXiv:1910.06376 [Cond-Mat] (2019).

This is the author's peer reviewed, accepted manuscript. However, the online version of record will be different from this version once it has been copyedited and typeset.

PLEASE CITE THIS ARTICLE AS DOI: 10.1063/1.50002168

13

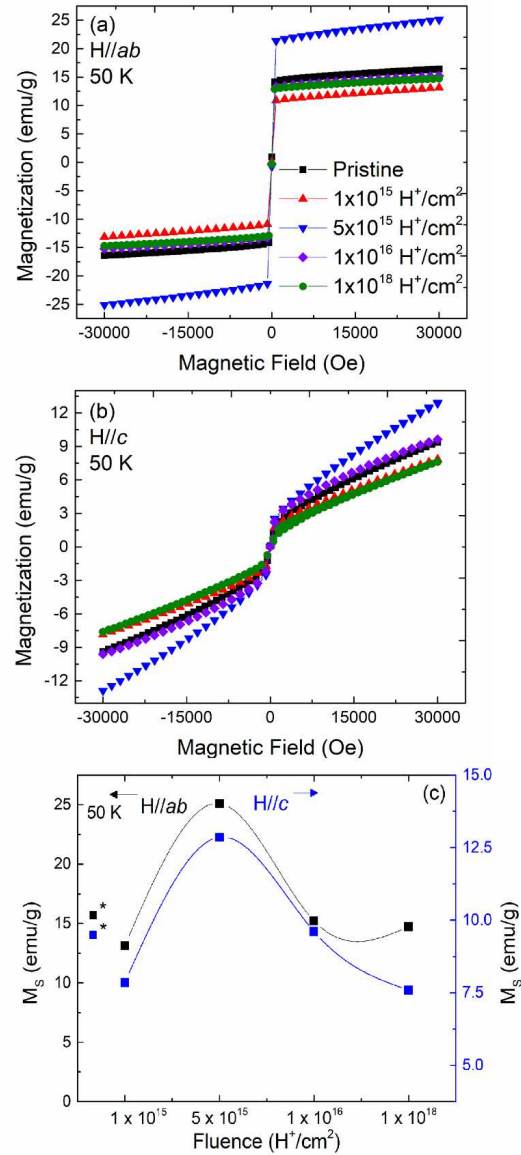


Figure 1: Isothermal magnetization measured in the ab plane (a), and in the c plane (b) performed in the ferrimagnetic phase at 50 K. The fluence dependent magnetization is shown; left y-axis represents the magnetization collected in ab plane, and the right y-axis shows the magnetization collected in c plane (c).

This is the author's peer reviewed, accepted manuscript. However, the online version of record will be different from this version once it has been copyedited and typeset.

PLEASE CITE THIS ARTICLE AS DOI: 10.1063/1.50002168

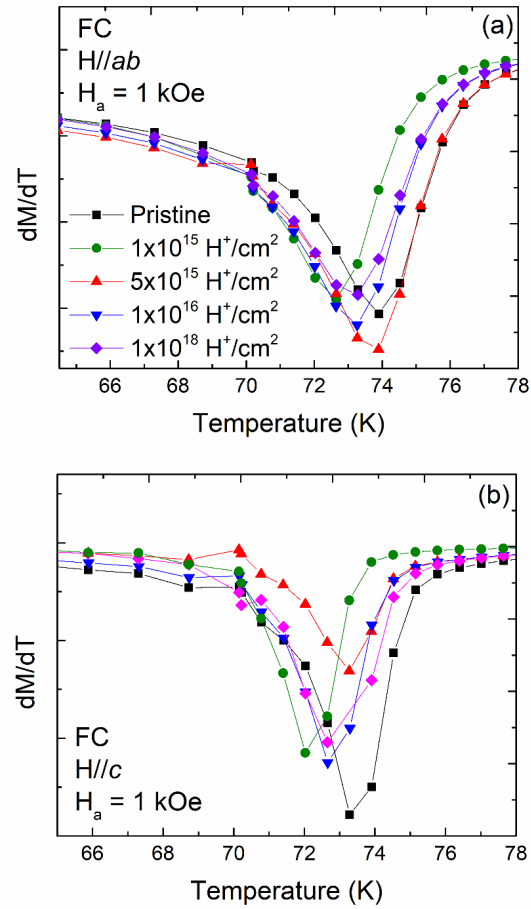


Figure 2: dM/dT curves obtained from magnetization vs temperature curves for pristine and all the proton fluence applied to MST. The curves are presented in both the out-of-plane (a) and the in-plane direction (b) from the Field-Cooled (FC) curves measured with an applied field of 1 kOe.

This is the author's peer reviewed, accepted manuscript. However, the online version of record will be different from this version once it has been copyedited and typeset.

PLEASE CITE THIS ARTICLE AS DOI: 10.1063/1.50002168

15

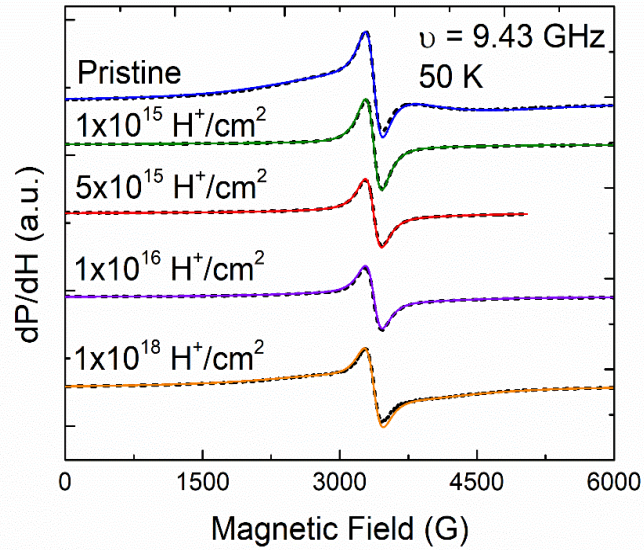


Figure 3: X-band (9.43 GHz) first derivative EPR spectra measured in the ferrimagnetic phase at 50 K for pristine and the proton irradiated MST crystals as a function of fluence. continuous curves are the computer-generated fits to the experimental signal shown in dotted curves.

This is the author's peer reviewed, accepted manuscript. However, the online version of record will be different from this version once it has been copyedited and typeset.

PLEASE CITE THIS ARTICLE AS DOI: 10.1063/5.0002168

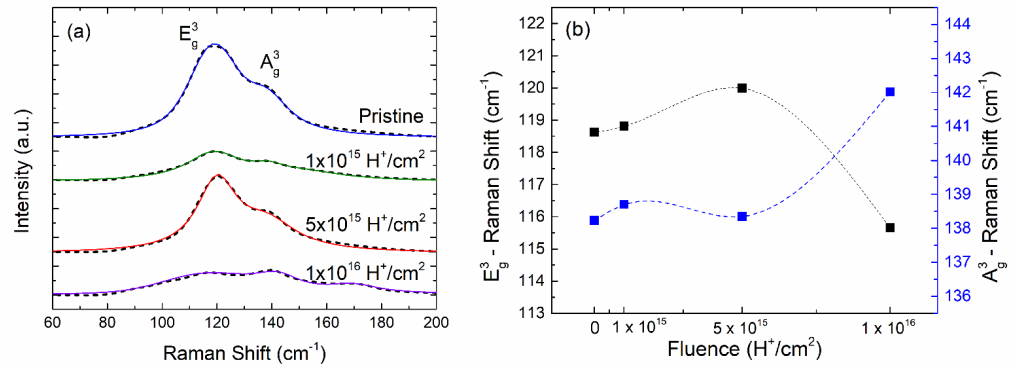
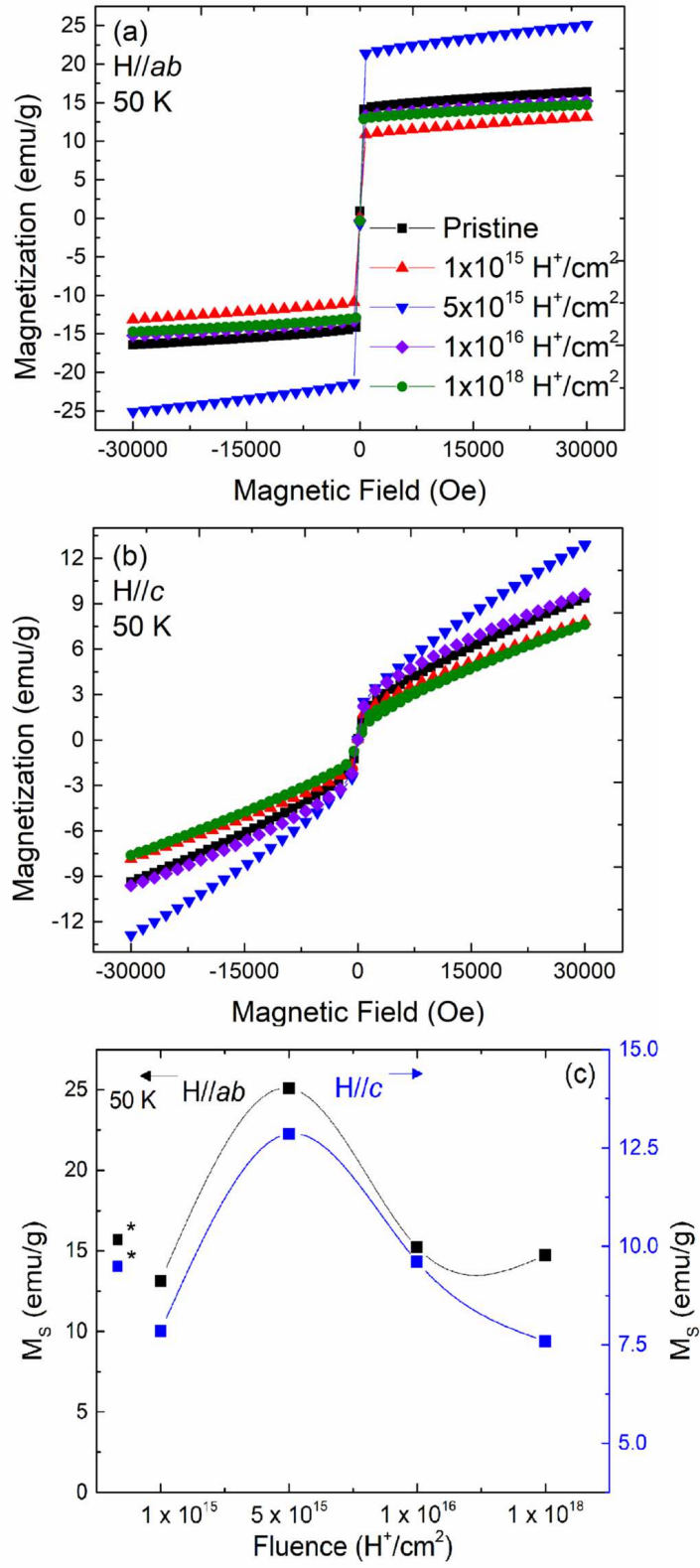


Figure 4: Raman spectra collected from pristine and proton irradiated MST as a function of fluence; dotted curves are experimental, and the continues curves are the fits employing Voigt lineshape (a); the peaks shift (including the Raman peak positions for the pristine MST crystal) derived from the fits as a function of proton fluence (b). The room temperature Raman data for $1 \times 10^{18} \text{ H}^+/\text{cm}^2$ is not available at this point.

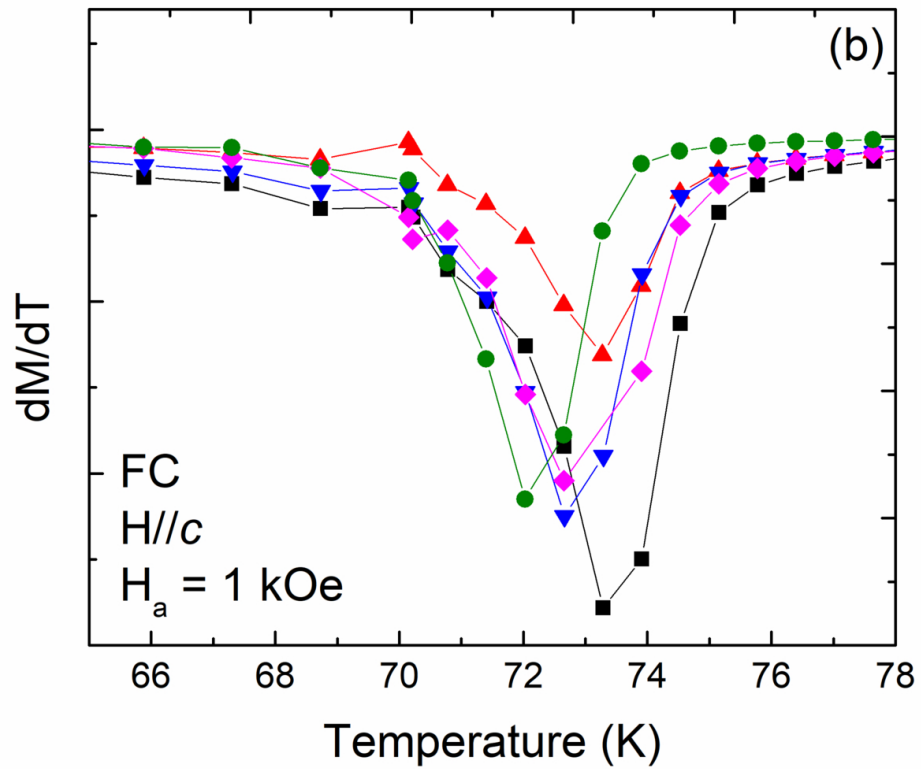
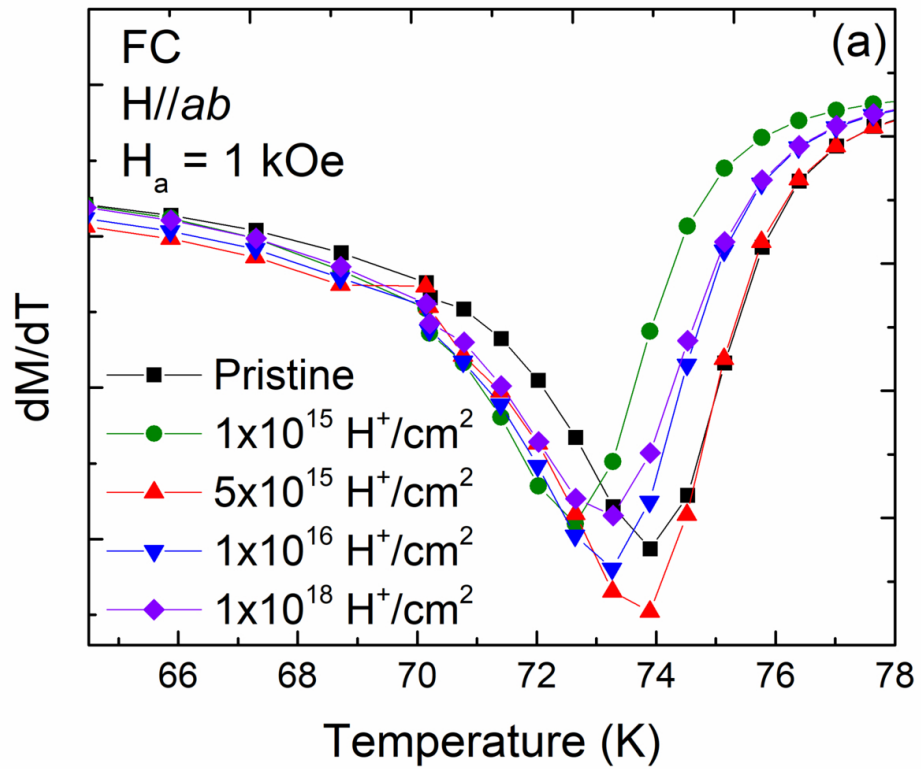
This is the author's peer reviewed, accepted manuscript. However, the online version of record will be different from this version once it has been copyedited and typeset.

PLEASE CITE THIS ARTICLE AS DOI: 10.1063/1.50002168



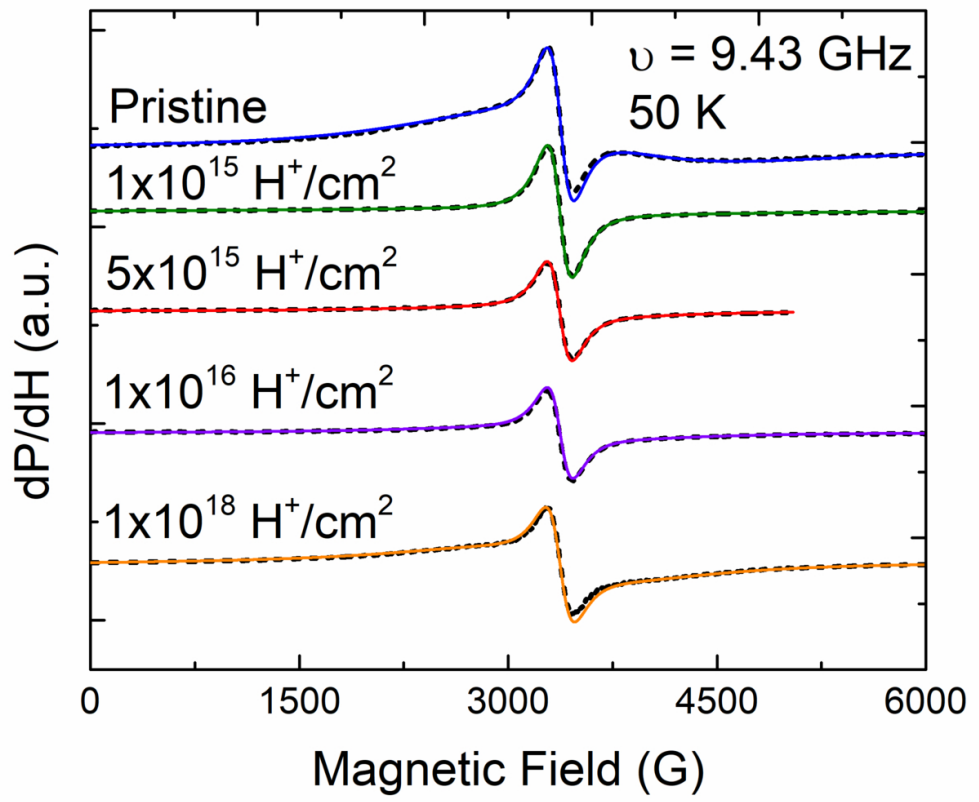
This is the author's peer reviewed, accepted manuscript. However, the online version of record will be different from this version once it has been copyedited and typeset.

PLEASE CITE THIS ARTICLE AS DOI: 10.1063/1.50002168



This is the author's peer reviewed, accepted manuscript. However, the online version of record will be different from this version once it has been copyedited and typeset.

PLEASE CITE THIS ARTICLE AS DOI: 10.1063/5.0002168



This is the author's peer reviewed, accepted manuscript. However, the online version of record will be different from this version once it has been copyedited and typeset.

PLEASE CITE THIS ARTICLE AS DOI: 10.1063/1.50002168

